

Spectroscopic characterization of rovibrational temperatures in atmospheric pressure He/CH₄ plasmas

Se Youn Moon, D. B. Kim, B. Gweon, and W. Choe^{a)}

Department of Physics, Korea Advanced Institute of Science and Technology, 335 Gwahangno, Yuseong-gu, Daejeon 305-701, Republic of Korea

(Received 17 June 2008; accepted 29 September 2008; published online 28 October 2008)

Atmospheric pressure of helium (He) and methane (CH₄) mixture discharge characteristics are investigated using emission spectroscopic methods. Plasmas are produced in a radio frequency capacitively coupled device at atmospheric pressure in the ambient air. Without the CH₄ gas introduced in the plasma, the emission spectrum exhibits typical helium discharge characteristics showing helium atomic lines with nitrogen molecular bands and oxygen atomic lines resulting from air impurities. Addition of a small amount (<1%) of CH₄ to the supplied He results in the emission of CN ($B^2\Sigma^+-X^2\Sigma^+$: violet system) and CH ($A^2\Delta-X^2\Pi$: 430 nm system) molecular bands. Analyzing the CN and CH diatomic molecular emission spectra, the vibrational temperature (T_{vib}) and rotational temperature (T_{rot}) are simultaneously obtained. As input power levels are raised from 20 W to 200 W, T_{vib} and T_{rot} are increased from 4230 K to 6310 K and from 340 K to 500 K, respectively. On the contrary, increasing the CH₄ amount brings about the decrease of both temperatures because CH₄ is harder to ionize than He. The emission intensities of CN and CH radicals, which are important in plasma processing, are also changed along with the temperature variation. From the results, the atmospheric pressure plasma shows strong nonequilibrium discharge properties, which may be effectively utilized for thermal damage free material treatments. © 2008 American Institute of Physics. [DOI: 10.1063/1.3002397]

I. INTRODUCTION

Atmospheric pressure plasmas have attracted great attention due to their many advantages.^{1–6} They have been studied for the possible in-line processes with high processing efficiencies especially in material processes, such as surface treatments, modifications, functionalization for biomedical applications, nanomaterial synthesis, and thin film depositions.^{3–6} In achieving the specific goals, a number of different atmospheric pressure plasma sources have been adopted. By utilizing various bias frequencies from direct current (dc) to microwave, a wide variety of plasma sources have been attempted including corona discharges, microdischarge plasmas, capacitively coupled plasmas, hollow cathode discharges, dielectric barrier discharges, jet-type plasmas, etc.^{1,4,5,7,8} In addition, many processes use molecular gases, such as CH₄, C₂H₂, N₂, CF₄, and so on for their unique purposes.^{4–9} In the molecular gas discharges, plasmas can lead to molecule decompositions, radical generations, and molecular excitation of electronic and rovibrational states which strongly affect the material qualities.^{9,10} Therefore, it is necessary not only to study the material properties but also to investigate the properties of the atmospheric pressure plasmas, which may serve as essential information for the control of the processing rate and its efficiencies. Among the plasma parameters, temperatures are relevant to the chemical reactivity and particle kinetics of the molecules existing in the plasmas. Low gas temperature, especially, is one of the most important features in the treatment of thermally

sensitive films, such as organic tissues and biocompatible materials.^{3,11}

In diagnosing the atmospheric pressure plasma characteristics, the spectroscopic methods are frequently favored.^{12,13} An optical spectrum emitted from the plasma provides some important information, such as the identification of existing species like atoms, molecules, and radicals, and also plasma temperatures and electron density.¹⁴

In this work, the spectroscopic diagnostics of atmospheric pressure plasmas using He and CH₄ mixture are performed, of which gas composition is widely used for amorphous hydrogenated carbon (*a*-C:H) coatings, generation of carbon nanotubes, and hydrophobic treatment of surfaces. In addition, the effects of input power and gas addition on temperatures are investigated.

II. EXPERIMENTAL SETUP

Figure 1 depicts a schematic illustration of the experimental setup under study. The discharge source has two parallel copper electrodes with the same diameters of 60 mm, cooled by chilled water. The discharge gap between the electrodes is fixed at 4 mm for stable plasma generation. The bottom electrode is powered by a 13.56 MHz rf supply (Dressler Cesar 1312) through an impedance matcher. The electrical signals of root-mean-square voltage (V_{rms}) and current (I_{rms}) are measured by a voltage probe (Tektronix P6051A), a current probe (Tektronix TCP 202), and a digital oscilloscope (Tektronix TDS 3012), as indicated in Fig. 1. The gas supplied for the experiment is a mixture of helium and methane with helium gas flow rate fixed at 3 standard liters per minute (slpm) and the methane gas added to it from

^{a)} Author to whom correspondence should be addressed. Electronic mail: wchoe@kaist.ac.kr.

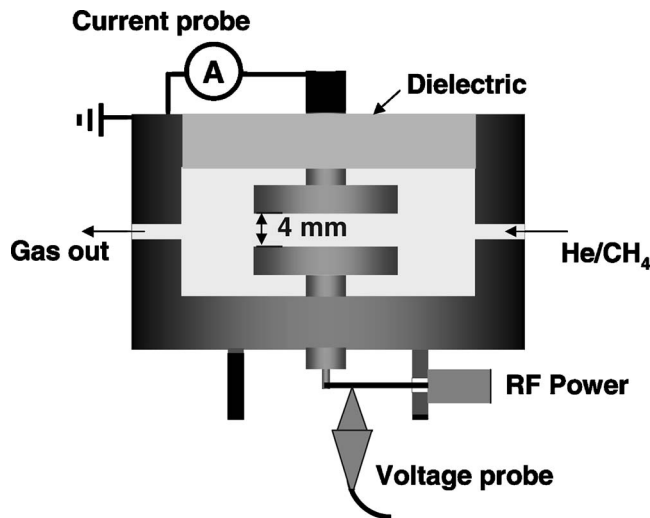


FIG. 1. Schematic illustration of the experimental setup for atmospheric pressure He/CH₄ discharge.

0 to 30 standard cubic centimeters (sccm) using a mass flow controller. However, the plasma was generated in the ambient air. In the experiments, the gas pressure is always fixed at 760 Torr (101 325 Pa) as flowing helium or mixed gas using pressure instruments (Pfeiffer Vacuum, Piezo gauge APR260, single gauge reader TPG261). Optical emission spectra are obtained using a visible spectrometer (Chromex 250is) and relevant optics.

III. RESULTS AND DISCUSSIONS

Figure 2 shows the typical emission spectra of helium discharge (top) and helium-methane mixture discharge (bottom) in the wavelength range of 330–480 nm and 480–800 nm, respectively. Both discharges emit not only helium atomic lines but also nitrogen molecular bands and oxygen atomic lines.¹⁵ They originated from ambient air impurities that are introduced through an opening in the discharge system. Although the nitrogen molecular emission band, N₂ first positive system which has a bandhead at 670.4 nm for (5,2) transition, appears around 667.8 nm, the atomic helium line (667.8 nm) is more remarkable as seen in Fig. 2(b). One of the important features of CH₄ addition is the occurrence of CN (*B*²Σ⁺-*X*²Σ⁺, 388.3 nm), CH (*A*²Δ-*X*²Π, 431.4 nm) molecular emission bands and hydrogen atomic line (H_α, 656.3 nm) as a subproduct from CH₄ decomposition.^{9,10,16} However, no significant differences in other spectral ranges are observed. The CN radicals (activation energy, *E*_a = 3.2 eV) are produced via reactions between methane and nitrogen atoms from air impurities, and CH radicals (*E*_a = 2.9 eV) appear through the electron impact dissociative excitation of CH₄ molecules as the most probable reaction paths,^{9,10,16,17}

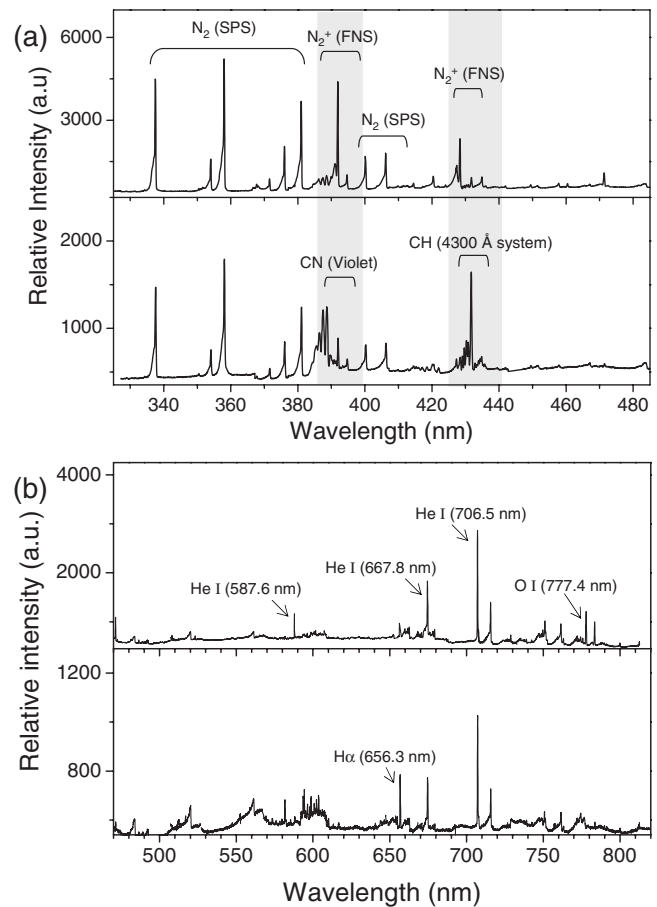
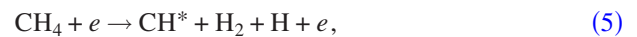
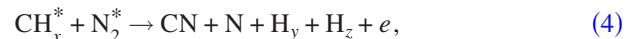


FIG. 2. (a) Emission spectra from 300 nm to 480 nm and (b) from 480 nm to 800 nm for the helium discharge (top) and the He/CH₄ discharge (bottom) at 100 W.



where $x=y+z$ and superscript (*) represents the excited states.

In the thin film growth, especially, CH radicals play a significant role with an important sticking coefficient due to three dangling bonds.^{9,10,16} Although the nitrogen molecular bands (N₂⁺ first negative system) show intense emission in the helium discharge as depicted in Fig. 2(a), they appear much less prominent as CH₄ is added due to the relatively strong CN and CH emissions, as depicted in Fig. 2(b). This suggests that both CN and CH spectra can be used as a thermometer.

In order to obtain the vibrational temperature (*T*_{vib}) and rotational temperature (*T*_{rot}), both CN and CH spectra are investigated using the well-known synthetic method.^{12,18–20} It is known that *T*_{vib} provides the information of the energy transfer between electrons and heavy particles, especially molecules, which shows the similar tendency with the electron temperature.^{13,18} On the other hand, measurement of *T*_{rot} is important to estimate gas temperature in atmospheric pressure plasmas due to the sufficiently fast rotational-translational relaxation.^{11,12,21}

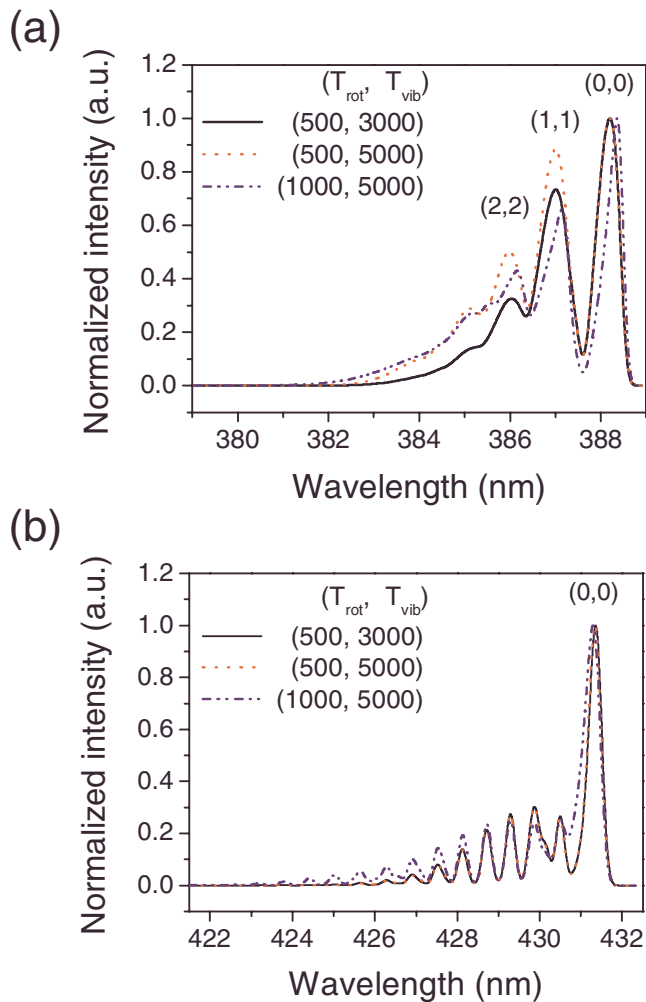


FIG. 3. (Color online) (a) Synthetic CN (violet system) and (b) CH (430 nm system) spectra at various T_{vib} (3000 K and 5000 K) and T_{rot} (500 K and 1000 K).

Figure 3 describes the temperature effect on the synthetic spectra of CN and CH, respectively. They are normalized with respect to each bandhead intensity and are obtained with the same Gaussian-shaped line broadening width of 0.1 nm which is mainly attributed from the instrumental broadening.^{12,13} As shown in Fig. 3(a), the most prominent band in the CN molecular spectrum comes from the $(v', v'')=(0, 0)$ of $\Delta v=0$ transition, and it overlaps with other $\Delta v=0$ transition bands from $(v', v'')=(1, 1)$ to (5,5). The bands are selected due to their available strengths as shown in Fig. 2. Since the spectral features are strongly influenced by the changes in T_{vib} and T_{rot} , both temperatures can be determined simultaneously. On the other hand, in the CH synthetic spectrum as seen in Fig. 3(b), only two vibrational transitions (0-0) and (1-1) are considered due to the intensity limitation of the range of interest near 431 nm. As shown in the black and red curves, the change in the emission spectrum due to the different T_{vib} is small, which suggests that the CH spectra can be used for accurate measurement of T_{rot} .

In Fig. 4, the results through comparing the experimental spectrum with the synthetic spectrum having the instrumental broadening width of 0.22 nm using the minimum χ^2

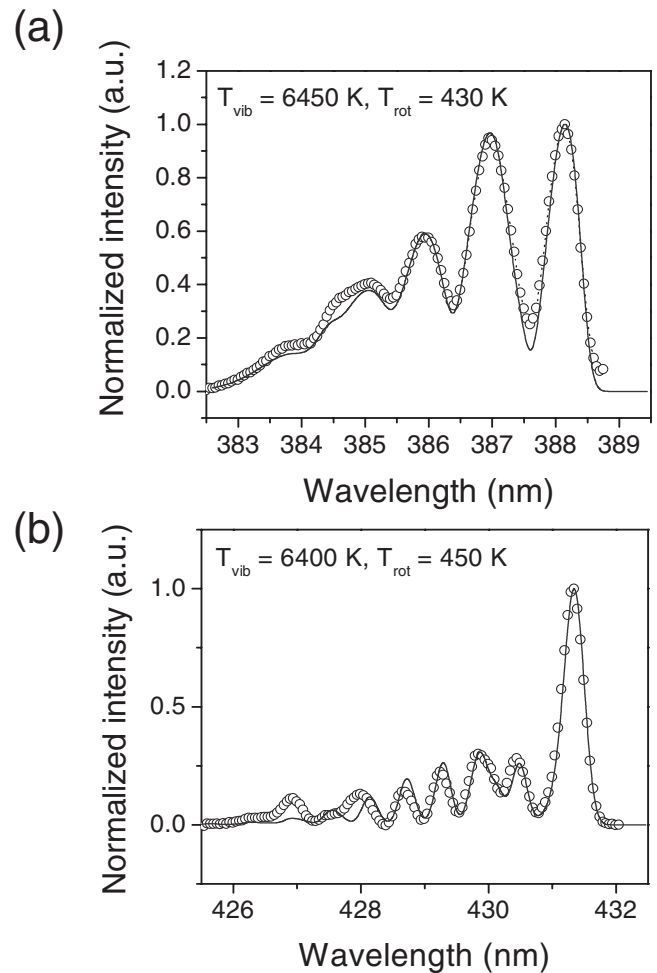


FIG. 4. Comparison between synthetic spectrum (—) and experimental spectrum (-○-) for (a) CN emission and (b) CH emission.

method are presented.^{12,19} The value of χ^2 is determined as follows:

$$\chi^2 = \sum_{i=1}^N \frac{(I_i^{\text{exp}} - I_i^{\text{syn}})^2}{N(N-1)}, \quad (6)$$

where I_i^{exp} and I_i^{syn} represent the experimental and synthetic spectral intensities of the i th datum of the N point spectrum, respectively. As depicted in the figure, the experimental spectra are in good agreement with the synthetic spectra. At 100 W input power and 10 sccm CH_4 addition, the values of $(T_{\text{vib}}, T_{\text{rot}})$ are obtained as (6450 K, 430 K) and (6400 K, 450 K) by the CN and CH spectra, respectively, which demonstrates only a 0.4% difference in T_{vib} and a 2.5% difference in T_{rot} . This small difference is attributed from the discrepancy between the synthetic and the experimental CH spectra below 428 nm as shown in Fig. 4(b). This is due to the blending of nitrogen molecular band (N_2^+ , first negative system) with the bandhead at 427.8 nm as observed in Fig. 2(a).

By varying the discharge conditions, such as input power levels from 50 W to 200 W and CH_4 amounts from 10 sccm to 30 sccm, changes in the temperatures and the emission intensity of CH bandhead (431.4 nm), CN bandhead (388.3 nm), and helium atomic line (706.5 nm) are also

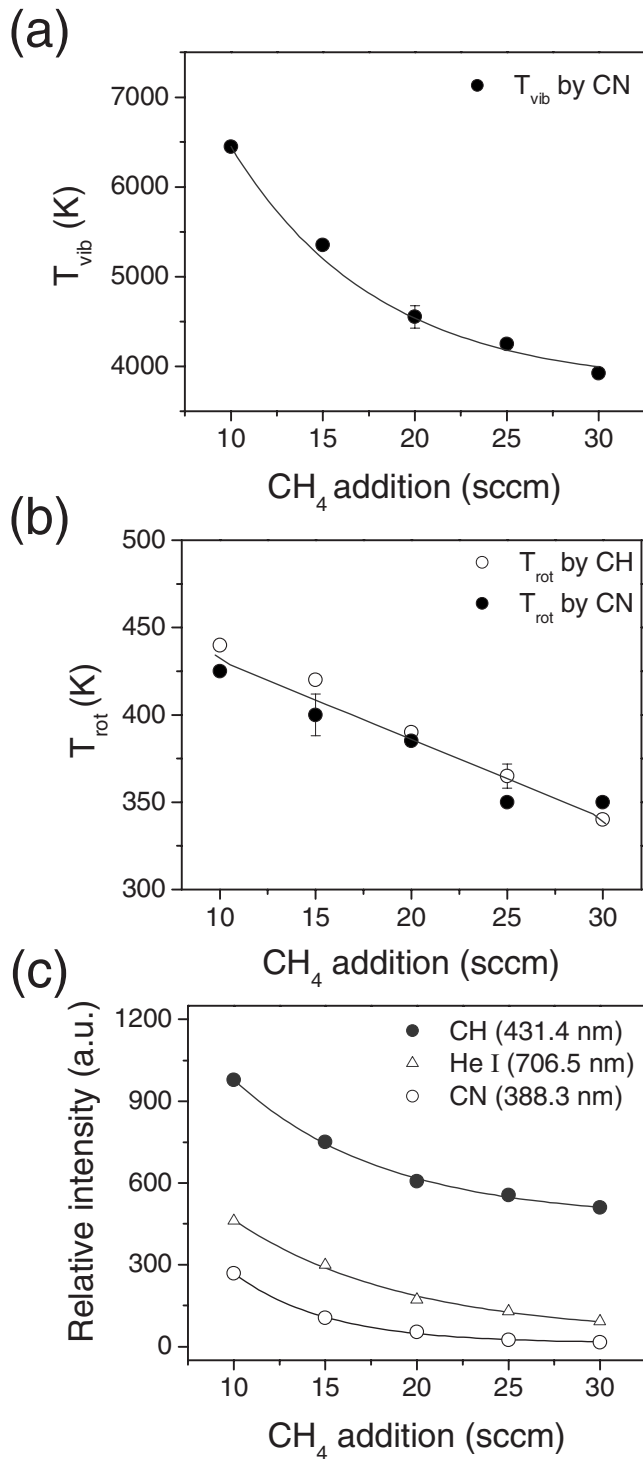


FIG. 5. Effects of CH₄ additions on the (a) T_{vib} , (b) T_{rot} , and (c) emission intensities of CH, He I, and CN spectral lines.

investigated, and the results are presented in Figs. 5 and 6. This may be used as important information in the practical application, such as for control of material processing or deposition rate^{9,10,16} with a reasonable time resolution as the process proceeds while the plasma parameters change during the specific process, such as film growth. The error bars shown in Figs. 5 and 6 are based on statistical treatment of the several repeatedly conducted experimental data.

First of all, only a small addition of CH₄ to the feeding

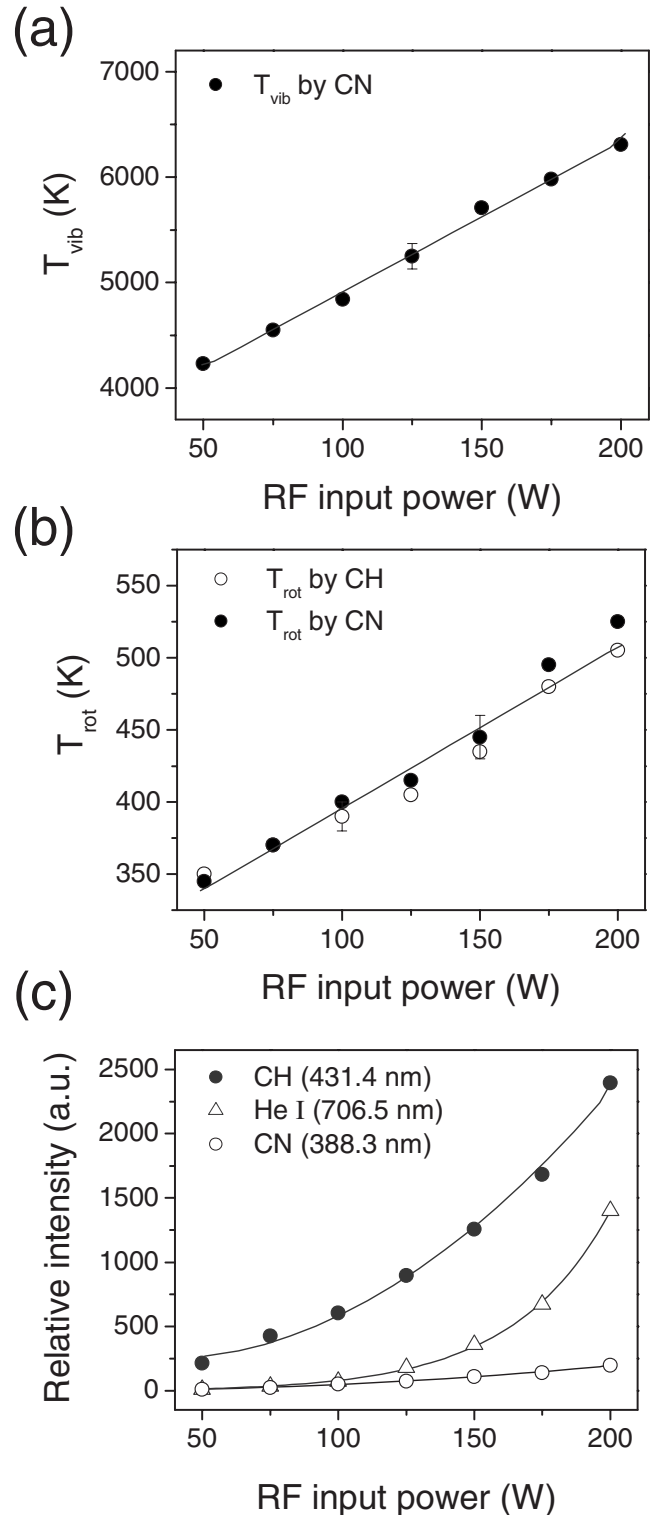


FIG. 6. Effects of rf input power on the (a) T_{vib} , (b) T_{rot} , and (c) emission intensities of CH, He I, and CN spectral lines.

He gas brought about significant changes both in T_{vib} and T_{rot} . As the CH₄ flow is raised from 10 sccm (0.3%) to 30 sccm (1% of the He supply), T_{vib} and T_{rot} are decreased from 6450 K to 3920 K and 430 K to 345 K, respectively, as described in Figs. 5(a) and 5(b). Since it is hard to know the exact ionization, excitation, and dissociation rates at atmospheric pressure due to the lack of enough information on

electron kinetics, we just compare the breakdown voltage to indirectly find the additive CH₄ effects on temperatures. From the electrical measurements, the breakdown voltage for the gas discharge is increased from 450 V_{rms} to 550 V_{rms}, and the power coupling efficiencies are lowered. This is because CH₄ is harder to ionize than He (of which breakdown voltage is 400 V_{rms} at the same conditions) at atmospheric pressure. This is also confirmed by the decrease of emission intensities as seen in Fig. 5(c).

Raising the rf input power from 50 W to 200 W at fixed 20 sccm CH₄ and 3 slpm He, on the other hand, increases both temperatures [Figs. 6(a) and 6(b)] and emission intensities [Fig. 6(c)] due to more energetic electrons and increasing collisions between particles. As shown in Figs. 5(c) and 6(c), the intensity of CN is always lower than that of CH, which is different from other experimental results using methane-nitrogen discharges.^{9,10} Since only a little amount of nitrogen gas exists in the chamber in our experiment, the CH radical has higher intensity and stronger dependence on the operational conditions.

From the results, the simultaneously determined T_{rot} by both CN and CH spectra shows the values within 2.5% error, which suggests that the two species can be used as thermometers in methane aided plasmas. Since CN or CH radicals play important roles in material processing, the control of concentrations and plasma temperatures is very important. From the intensity measurement, it is shown that the relative radical concentrations of CN and CH are controlled by various operational conditions because the emission intensity depends largely on the radical concentration.^{9,14,22,23} The experimental results in this work clearly demonstrate that the gas flow rate and the input power are two main control parameters for relative concentration of radicals and adequate plasma temperatures. In addition, the measured values of T_{vib} and T_{rot} in our atmospheric pressure rf discharges suggest that the material processing of thermally sensitive materials can be possible with high chemical reactivity and low thermal damage under different operating conditions.

IV. SUMMARY

Atmospheric pressure He/CH₄ plasmas are produced and their spectroscopic plasma properties are investigated using optical emission diagnostics. The addition of a small amount of CH₄ to the supplied He gas mainly changes the CN (388.3 nm) and CH (431.4 nm) molecular emission spectra. Using the two spectra, T_{vib} and T_{rot} are obtained under various operating conditions. While increasing the input power level from 50 W to 200 W, both T_{vib} and T_{rot} are

increased from 4230 K to 6310 K and from 340 K to 500 K, respectively. However, as the methane addition is increased, T_{vib} and T_{rot} are decreased from 6450 K to 3920 K and 430 K to 345 K, respectively. From the temperature measurements, it is shown that the atmospheric pressure He/CH₄ plasma is in the highly nonthermal equilibrium state of relatively low rotational temperature, suggesting that the thermally sensitive material treatments are possible with high chemical reactivity. In addition, the effects of gas compositions and input power are investigated, and the result shows that the plasma properties can be controlled by operating conditions to obtain the required plasma temperatures.

ACKNOWLEDGMENTS

This work was partly supported by the Korea Institute of Machinery and Materials.

- ¹S. Y. Moon, W. Choe, and B. K. Kang, *Appl. Phys. Lett.* **84**, 188 (2004).
- ²C. Tendero, C. Tixier, P. Tristant, J. Desmaison, and P. Leprince, *Spectrochim. Acta, Part B* **61**, 2 (2006).
- ³S. Y. Moon, J. W. Han, and W. Choe, *Thin Solid Films* **506**, 355 (2006).
- ⁴S. H. Kim, J. H. Kim, B. K. Kang, and H. S. Uhm, *Langmuir* **21**, 12213 (2005).
- ⁵C. Sarra-Bournet, S. Turgeon, D. Mantovani, and G. Laroche, *J. Phys. D* **39**, 3461 (2006).
- ⁶H. Shirai, T. Kobayashi, and Y. Hasegawa, *Appl. Phys. Lett.* **87**, 143112 (2005).
- ⁷D. B. Kim, J. K. Rhee, B. M. Gweon, S. Y. Moon, and W. Choe, *Appl. Phys. Lett.* **91**, 151502 (2007).
- ⁸A. Yanguas-Gil, K. Focke, J. Benedikt, and A. von Keudell, *J. Appl. Phys.* **101**, 103307 (2007).
- ⁹J. Pereira, V. Massereau-Guilbaud, I. Géraud-Grenier, and A. Plain, *Plasma Chem. Plasma Process.* **2**, 633 (2005).
- ¹⁰S. V. Avtaeva and T. M. Lapochkina, *Plasma Processes Polym.* **33**, 774 (2007).
- ¹¹E. Stoffels, I. I. Kieft, and R. E. J. Sladek, *J. Phys. D* **36**, 2908 (2003).
- ¹²S. Y. Moon and W. Choe, *Spectrochim. Acta, Part B* **58**, 249 (2003).
- ¹³O. Motret, C. Hibert, S. Pellerin, and J. M. Pouvesle, *J. Phys. D* **33**, 1493 (2000).
- ¹⁴W. Lochte-Holtgreven, *Plasma Diagnostics* (AIP, New York, 1968).
- ¹⁵S. Y. Moon, J. K. Rhee, D. B. Kim, and W. Choe, *Phys. Plasmas* **13**, 033502 (2006).
- ¹⁶K. J. Clay, S. P. Speakman, G. A. J. Amaratunga, and S. R. P. Silva, *J. Appl. Phys.* **79**, 7227 (1996).
- ¹⁷S. Bhattacharya, A. Granier, and G. Turban, *J. Appl. Phys.* **86**, 4668 (1999).
- ¹⁸G. Herzberg, *Molecular Spectra and Molecular Structure: I. Spectra of Diatomic Molecules*, 2nd ed. (Van Nostrand, Princeton, 1964).
- ¹⁹S. Acquaviva, *Spectrochim. Acta, Part A* **60**, 2079 (2004).
- ²⁰J. Luque and D. R. Crosley, *J. Chem. Phys.* **104**, 2146 (1996).
- ²¹S. Pellerin, J. M. Cormier, F. Richard, K. Musiol, and J. Chapelle, *J. Phys. D* **29**, 726 (1996).
- ²²M. Hiramatsu, K. Kato, C. H. Lau, J. S. Foord, and M. Hori, *Diamond Relat. Mater.* **12**, 365 (2003).
- ²³P. Chabert, H. Abada, J. P. Booth, and M. A. Lieberman, *J. Appl. Phys.* **94**, 76 (2003).